

An Experimental Investigation into Improving the Performance of Thermoelectric Generators

Ali Alahmer¹, Mohammad Bani Khalid², Nabil Beithou^{1,2}, Gabriel Borowski³, Sameh Alsaqoor^{1*}, H. Alhendi⁴

¹ Department of Mechanical Engineering, Tafila Technical University, P. O. Box 179, 66110, Tafila, Jordan

² Department of Mechanical and Industrial Engineering, Applied Science Private University, P.O.Box 166, 11931, Amman, Jordan

³ Faculty of Environmental Engineering, Lublin University of Technology, ul. Nadbystrzycka 40B, 20-618 Lublin, Poland

⁴ Department of Civil Engineering, Applied Science Private University, P.O.Box 166, 11931, Amman, Jordan

* Corresponding author's e-mail: sameh@wp.pl

ABSTRACT

Low-temperature heat sources have become increasingly popular in recent years, particularly for energy generation. The majority of thermal devices in the market (including devices using solar energy, geothermal energy, waste energy, and so on) transform heat into electricity indirectly, requiring mechanical work before producing power. Through the Seebeck effect, the technology that employs a thermoelectric generator (TEG) may directly transform heat energy into electricity. The TEG technology provides several advantages, including compactness, quietness, and the absence of moving components. TEGs have a low thermal and electrical efficiency, which is one of their main drawbacks. Therefore, the performance of a thermoelectric generator is improved by employing liquid evaporation heat transfer in this manuscript. The performance of the thermoelectric was examined experimentally and compared to the liquid evaporation mode under varied heat flux values and different modes of heat transfer in terms of free and forced convection with and without fins. The experimental results revealed that when compared to free convection without fins, adopting forced liquid evaporation convection would improve TEG voltage variation by 435.9%.

Keywords: thermoelectric generator, liquid evaporation, TEG performance, enhancing power generation, waste energy harvesting.

INTRODUCTION

Energy harvesting systems have received substantial interest as a result of the increase in energy consumption. Researchers are stepping up their attempts to find new energy sources or concentrating on the development of energy harvesting-based electricity generation which are simple to use and characterized by high productiveness. Thermoelectric generators (TEGs) are semiconductor devices that have exhibited their capacity to transform thermal energy directly into electrical energy via one of three thermoelectric criteria [Aridi et al. 2021]: the Seebeck effect, Peltier

effect or Thomson effect. The Seebeck effect is the transformation of a temperature variation to power generation; the Peltier effect is the production of temperature differential at the joint of two distinct materials by an electric current, and the Thomson effect is an adaptation of the Peltier–Seebeck model. To summarize, the current is the driving effort to heat in the Peltier effect, whereas the difference in heat is the driving effort to the current in the Seebeck effect. Thermoelectric generators (TEGs) have received special attention in the realm of energy harvesting in recent years, with applications ranging from large scale to tiny, depending on size, supplied power, and materials

utilized. TEGs are widely employed in a variety of areas due to their appealing characteristics, which include energy economy, low maintenance, manufactured out of a variety of materials, including silicon, ceramics, and polymers, a suitable option for low-power systems with limited electrical grid access, and a long lifespan [Jaziri et al. 2020, Dell et al. 2019]. On the other hand, TEG has a low efficiency of less than 7% [Chen et al. 2017]. Many factors influence the TEG efficiency, including [Snyder and Toberer 2011, Polozine et al. 2014]: (i) thermoelectric properties of the material in terms of thermal conductivity K , Seebeck coefficient, and resistivity, which should all be high, (ii) temperature gradient, which is influenced by the volume flow rate of the sink and the heat source, as well as properties of the heat input, flowing fluid, and heat exchanger configuration, (iii) The figure of merit (ZT) is a non-dimensional metric that represents overall performance and should be maximized.

Several studies have been published to examine the usage of thermoelectric generators for waste heat recovery, design configuration and optimization, and enhanced performance. Meng et al. [2017] investigated theoretically the possible development for close to 1.47 kW of electrical energy from a hot flow gas at 350 °C, with a generator efficiency of 4.5% and a payback period of about four years. Brset et al. [2017] demonstrated a thermoelectric generator used in a metal casting machine that absorbs energy from a 1400 °C hot side and delivers up to 160 W/m² of power output. Hadjistassou et al. [2013] conducted an analytical investigation on the efficiency of a thermoelectric generator and observed that it had a high efficiency of 5.29% at a thermal gradient of 324.6 K. Geometry optimization and Material optimization are the two most common research methodologies utilized to improve the TEG performance [Shittu et al. 2019]. Low thermal conductivity, high electrical conductivity, and a high Seebeck coefficient are required for optimal thermoelectric materials [Elsheikh et al. 2014]. In regard to structure optimization, Omer and Infield [1998] conducted a theoretical study of a thermoelectric generator, with a focus on thermoelectric leg length optimization. The results demonstrated that by improving the TEG shape, its power output may be increased. Araiz et al. [2020] optimized numerous parameters of the installation of the thermoelectric module on the exterior wall of a flue gas chimney to generate up

to 45 kW of electric power. The efficiency of thermoelectric generators may be boosted by using heat transfer enhancement devices. Heat pipe or liquid metal are extensively used to expel waste heat because of its low thermal resistance [Orr 2016]. Heat pipes with high thermal conductivity are placed on the adjoining cold and hot plates of TEG. Liquid metal was employed by Dai et al. [2011] to capture and transmit waste heat. Heat is transferred from the waste heat source to the TEG hot side through an electromagnetic pump. Cao et al. [2018] developed a thermoelectric generator with a heat pipe for recovering waste heat from automobile exhaust. The best thermoelectric device designs, including the better heat pipe installation thickness and the optimum angle between the gas flow direction and the heat pipe row, were tested using an experimental prototype. According to the results, the power output, optimized efficiency, and pressure drop are 13.08 W, 2.58%, and 1657 Pa, respectively.

Furthermore, many improved heat transfer structures are utilized to improve heat transmission, such as metal foams, phase change materials (PCMs), and metal fins. The heat sink duct is packed with metal foams to enhance the coefficient of heat transfer. The metal foams filling the heat sink duct were employed by Wang et al. [2016] to improve heat transmission on both sides of TEG. As a result, metal foams may significantly enhance the heat transfer coefficient on both the hot-air and water-cooling sides. In the TEG system, PCMs are also employed to improve temperature stability and power generation efficiency. Atouei et al. [2017] employed PCM and air cooling to improve the power generating efficiency. Rea et al. [2018] employed aluminum-silicon as the PCM to keep the temperature stable and store the heat. One of the most common techniques to improve heat transmission is to use a metal-fin heat sink. Araiz et al. [2021] studied experimentally the use of two thermoelectric generators for energy recovery from exhaust gases. Fins have been explored for the hot area heat exchangers. Two technologies have been developed for the cold side: an extended surfaces dissipater with a blower, which is commonly used in thermoelectric technologies, and a biphasic thermosyphon featuring free-convection, which seems to be a phase change mechanism that can work with no additional consumption. The results revealed that the thermoelectric generator with the finned dissipater produced a maximum net power of 6.9 W,

and the biphasic thermosyphon produced 10.6 W of electricity in the generator.

The main purpose of this paper was to employ several strategies to develop more efficient TEG devices. In particular, to employ liquid evaporation heat transfer experimentally to improve the performance of a thermoelectric generator. The thermoelectric performance was tested and compared to that of liquid evaporation under various heat flux values and diverse forms of heat transfer, including free convection, forced convection, free convection with fins, and forced convection with fins.

EXPERIMENTAL SETUP, EQUIPMENT AND PROCEDURE

Figure 1 illustrates a thermoelectric generator (TEG) that transforms temperature differences into electricity. The thermoelectric materials (properties of semiconductors) and temperature differences as displayed in Eq. 1 and 2 are primarily responsible for the power generated by TEG.

$$\dot{Q}_h = \alpha T_h I - \frac{1}{2} I^2 R + K (T_h - T_c) \quad (1)$$

$$\dot{Q}_c = \alpha T_c I + \frac{1}{2} I^2 R + K (T_h - T_c) \quad (2)$$

where: α is the Seebeck coefficient, R is the internal electrical resistance, K is the thermal conductance, I is current, T_h is the hot junction temperature, and T_c is the cold junction temperature.

The power generated by such a device may be computed using Eq. 3,

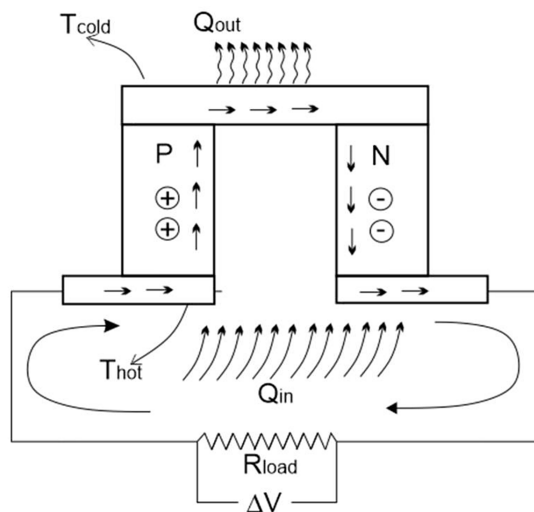


Figure 1. Thermoelectric generator model

$$P = \dot{W}_{net} = \dot{Q}_h - \dot{Q}_c \quad (3)$$

Moreover, the power can be found from Eq. 4,

$$P = V I \quad (4)$$

Eqs. 5 and 6 can be used to evaluate the thermal and Carnot efficiencies, respectively.

$$\eta_{th} = \frac{\dot{W}_{net}}{\dot{Q}_h} \quad (5)$$

$$\eta_{Carnot} = \frac{T_h - T_c}{T_h} \quad (6)$$

Thermoelectric modules can also be utilized for heating and cooling; however, the preceding equations must be modified accordingly. The heat transfer from TEG was explored in this experiment under various settings in order to improve the power provided by TEG. Natural and forced convection, finned surfaces, and liquid evaporation have all been investigated and tested. Experimental equipment incorporating TEG and sensing devices were set up to conduct these investigations. Figure 2 shows the experimental setup, which consists of:

- Variable power supply to regulate the voltage and current delivered to various devices in this test, such as the fan.
- A multimeter to measure the generated voltage difference from the TEG module.
- A thermoelectric generator of the TEG1-12611-08 type was used to evaluate its performance under various situations.
- Fan used in forced convection heat transfer.
- Thermocouples to monitor hot, cold, and ambient temperatures.

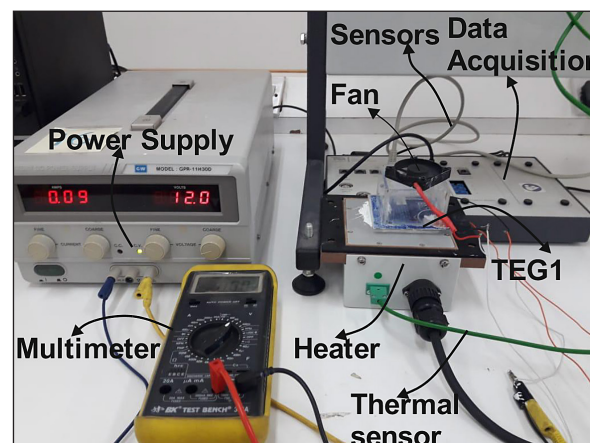


Figure 2. Real picture of the used device

- A variable heat flux supplying plate is used to supply varying heat flux levels to the TEG during the tests.
- Various electric wires for connections.

Figure 3 shows the employed TEG, which can generate 13 W at 300 °C, has a high temperature differential of up to 350 °C, and can generate 3A at full power. Table 1 lists the specifications of the TEG that was used.

In order to reduce the impact of contact thermal resistance, the was linked to the heat source and the thermal compound was applied to the hot surface of TEG [Angeline 2017]. The heat flux values used in these experiments are (1.4, 2.8, 4.2, and 5.6). A data acquisition system was used to capture heat flux, hot-side, cold-side, and ambient temperatures. The voltage difference induced by the TEG was measured with a multimeter.

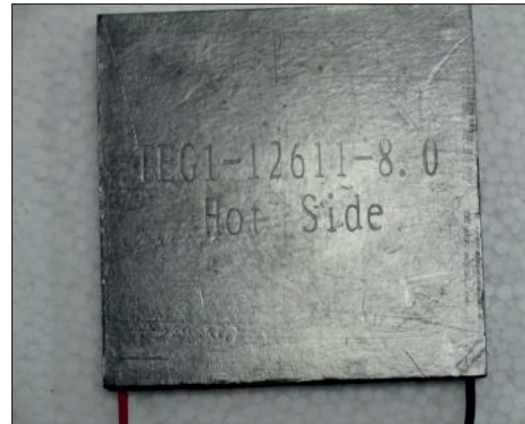


Figure 3. Used TEG module.

Table 1. The TEG module specifications

Open circuit voltage (V)	9.5
Match load resistance (Ω)	1.8
Match load output current (A)	2.7
Match load output power (W)	13

EXPERIMENTAL SCENARIO PERFORMED

Free and forced convection

As indicated in Figure 4, the experiment was set up for free then forced convection from a horizontal flat plate. The heat transfer from the top surface, which in the TEG represents the cold surface, may be computed using Newton law of cooling as follows:

$$\dot{Q} = h A (T_c - T_\infty) \quad (7)$$

where: h is the convection heat transfer coefficient, A is the TEG surface area ($5.6 \times 5.6 \text{ mm}^2$), and T_∞ is the ambient temperature. The heat transfer coefficient h can be found as:

$$h = \frac{Nu k}{L} \quad (8)$$

where: Nu is the Nusselt number, k is the thermal conductivity, and L is the characteristic length of the plate [Bergman 2011].

For free convection over a horizontal flat plate:

$$Nu = \left\{ 0.54 Ra^{\frac{1}{4}} \quad 10^4 < Ra < 10^7 \right. \quad (9)$$

$$Nu = \left\{ 0.15 Ra^{\frac{1}{3}} \quad 10^7 < Ra < 10^{11} \right. \quad (10)$$

For forced convection over a flat plate:

$$Nu = \left\{ 0.664 Re_L^{\frac{1}{2}} Pr^{\frac{1}{3}} \text{ laminar} \right. \quad (11)$$

$$Nu = \left\{ 0.0296 Re_L^{\frac{4}{5}} Pr^{\frac{1}{3}} \text{ turbulent} \right. \quad (12)$$

Figures 5 and 6 depict the temperature distribution and voltage difference for free and forced convection heat transfer from the TEG, respectively. Forced convection clearly increases heat transfer from the cold surface, hence increasing the temperature differential and voltage produced.

Forced convection resulted in a higher voltage difference, which indicates more power output, as demonstrated in Figures 5 and 6. Forced

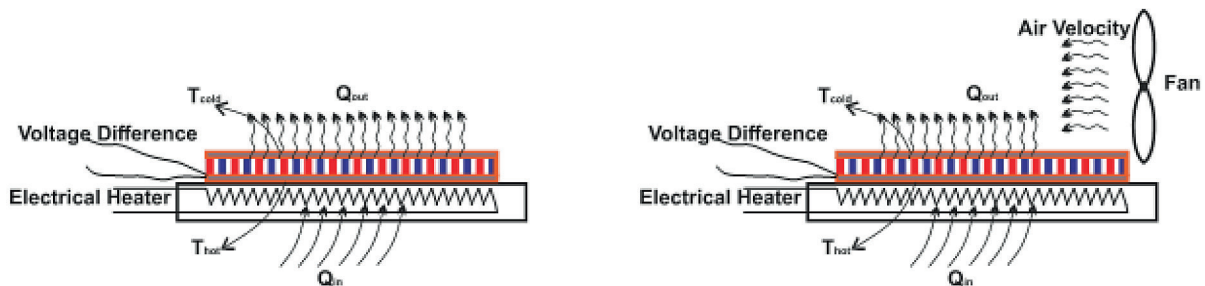


Figure 4. Schematic diagrams of the tested free and forced convection modes

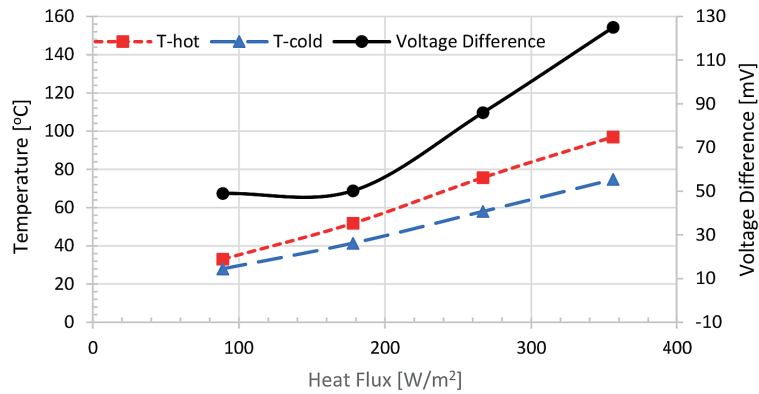


Figure 5. Temperatures and voltage variation versus heat flux for free convection mode

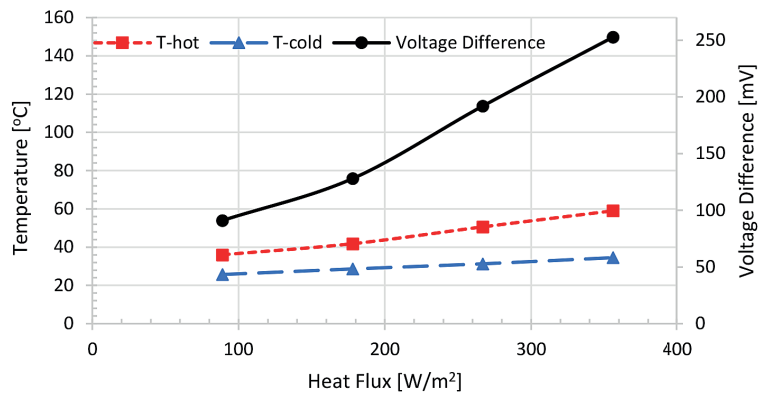


Figure 6. Temperatures and voltage variation versus heat flux for forced convection mode

convection improved TEG voltage variation by 116.5%, as compared to free convection.

Free and forced convection-finned surfaces

Extended surfaces can be utilized to promote the heat transfer from a cold surface and generate larger temperature differences. The thermoelectric module has been subjected to heating loads on the hot side and fins have been employed on the cold side to visualize the effect of finned heat transfer in both natural and forced modes, as presented in Figure 7. It shows rectangular fins, although any

type of expanded surface to improve heat transmission could be used instead.

Churchill and Chu correlation [1975] was used to calculate the natural convection heat transfer rate from a vertical finned surface:

$$Nu_L = \left\{ 0.825 + \frac{0.387 Ra_L^{\frac{1}{6}}}{\left[1 + (0.492/Pr)^{\frac{9}{16}} \right]^{\frac{8}{27}}} \right\}^2 \quad (13)$$

$$\dot{Q} = h A_t (T_b - T_{\infty}) \quad (14)$$

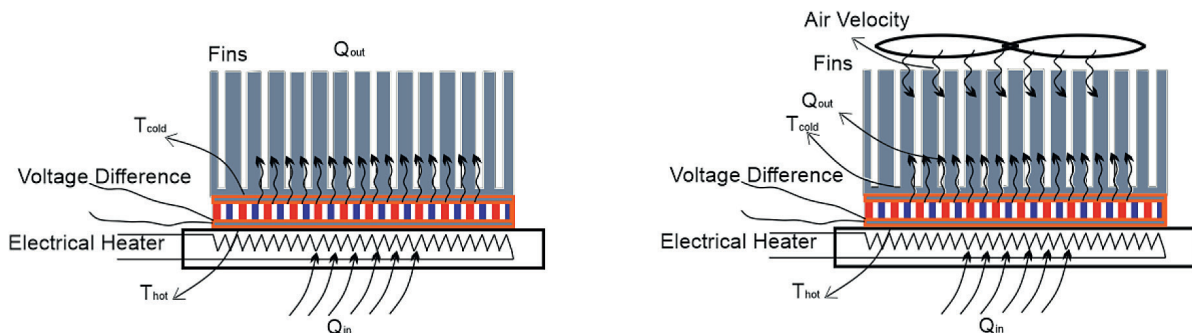


Figure 7. Schematic diagrams of the tested free and forced convection fin-modes

where: A_t is the total area base and fins,

$$A_t = N \eta_f A_f + A_b \quad (15)$$

$$\eta_f = \frac{\dot{Q}_f}{h A_f (T_b - T_\infty)} \quad (16)$$

$$\dot{Q}_f = M \tanh(m L_c) \quad (17)$$

$$m^2 = \frac{h P}{k A_c} \quad (18)$$

$$M = \sqrt{h P k A_c} (T_b - T_\infty) \quad (19)$$

where: P is the fin perimeter, k is the fin thermal conductivity, and A_c is the fin cross-sectional area.

Figure 8 compares the open circuit voltage for finned free and forced convection to plate free and forced convection. As predicted, employing expanded surfaces for both free and forced convection modes, results in a larger heat transfer rate.

Nonetheless, the authors tried to find a way to improve heat transmission from a cold surface while using the minimum resources possible. Liquid evaporative cooling is a potential method for passive high heat transfer from the cold surface of

the thermoelectric module. If a high heat transfer rate is obtained, the system's passive properties will be tested next. On average, free and forced convection with finned improved voltage variation of TEG by 119.8% and 288.4%, respectively, as compared to free convection without fins. Furthermore, forced convection with fins improved TEG voltage variation by 78.6% as compared to free convection with finned.

Free and forced convection-liquid evaporation

In the preceding sections, boosting heat transfer rate was accomplished through increasing air velocity and hence the heat transfer coefficient, as well as increasing the heat transfer surface area. In this section, the heat transfer method was switched from free and forced convection to liquid evaporative cooling. Ethanol C_2H_6O was chosen because of its lower boiling point (76 °C), as presented in Figure 9.

Eq. 20 was used to calculate the heat transfer rate while utilizing liquid evaporative

$$\dot{Q}_c = \dot{m}_{ev} h_{fg} = h_{T-ph} A (T_s - T_\infty) \quad (20)$$

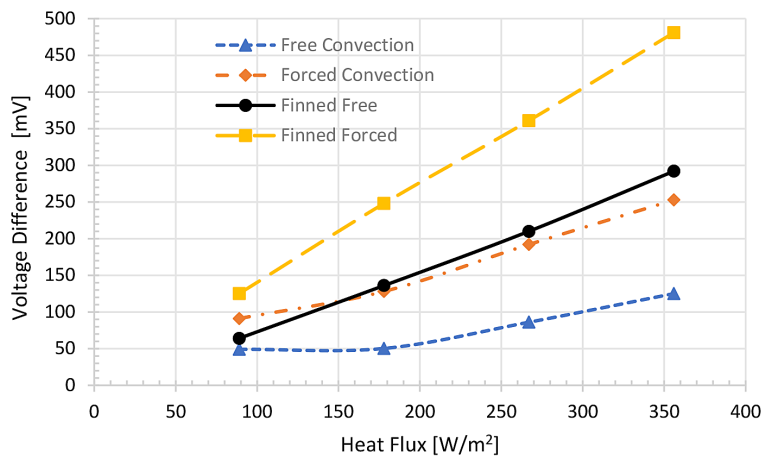


Figure 8. Open circuit voltage variation for free-forced finned-flat plate modes.

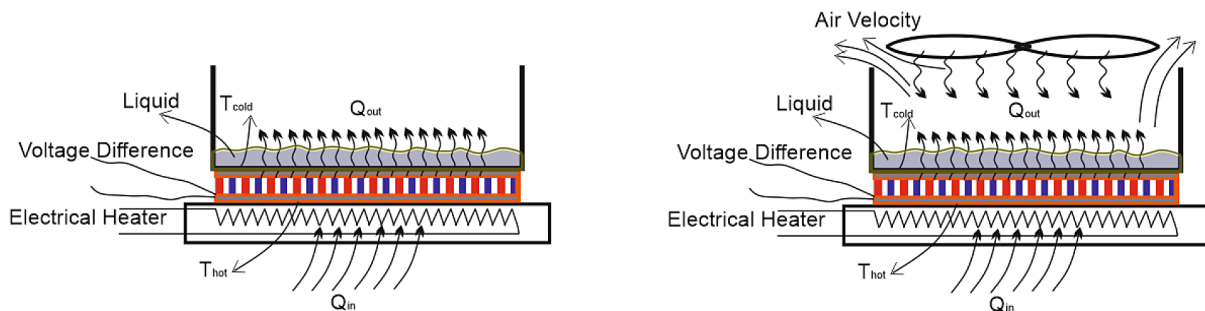


Figure 9. Schematic diagrams of the tested free and forced liquid evaporation-modes

where: \dot{m}_{ev} is the evaporation rate, h_{fg} is the latent heat of vaporization, and h_{T-ph} is the two-phase flow heat transfer coefficient.

The phase change heat transfer coefficient (HTC) is generally known to be substantially larger than the forced convection HTC [22]. The experiments on liquid evaporation in its liquid phase and nucleation stage were carried out. Figure 10 depicts the temperature differences between hot and cold surfaces, as well as the voltage differential, as a function of the heat input to the TEG. It is undeniable that liquid evaporation improves heat transmission; nevertheless, the improvement is not as significant as that of fin heat transfer. Figure 11 depicts the temperature differences between hot and cold surfaces, as well as the voltage differential, as a function of heat input for Liquid Forced Evaporation (LFE). The voltage differential increased dramatically, and the surface temperature dropped dramatically; the voltage was nearly tripled.

Figure 10 shows the hot and cold surfaces temperatures variation and the voltage difference

variation with different heat input (Liquid Free Evaporation).

Figure 11. shows the hot and cold surfaces temperatures variation and the voltage difference variation with different heat input (Liquid Forced Evaporation).

The voltages generated by the various heat transfer mechanisms are compared in Figure 12. As it can be seen, forced evaporative heat transfer was the most efficient option. During the experiments, much higher heat transfer rates were achieved, which can be attributed to the nucleate boiling that begins and increases the two-phase HTC. As a result, the surface temperature experienced a sudden drop and rise in value, as it moved from nucleate boiling to transition boiling before entering the film boiling stage. On average, free and forced liquid evaporation convection improved voltage variation of TEG by 73.8% and 435.9% as compared to free convection without fins. Moreover, forced liquid evaporation convection improved TEG voltage variation by 217.3%, as compared to free liquid evaporation convection.

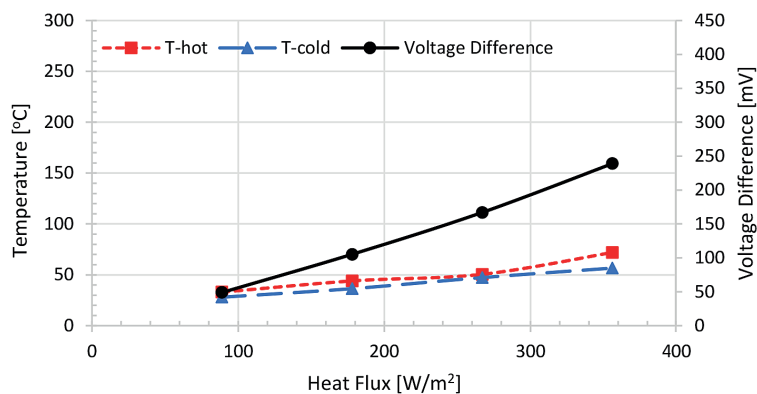


Figure 10. Liquid free evaporation

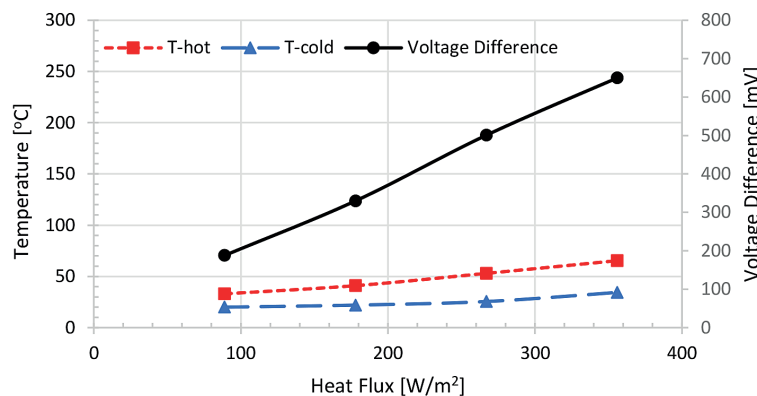


Figure 11. Liquid forced evaporation

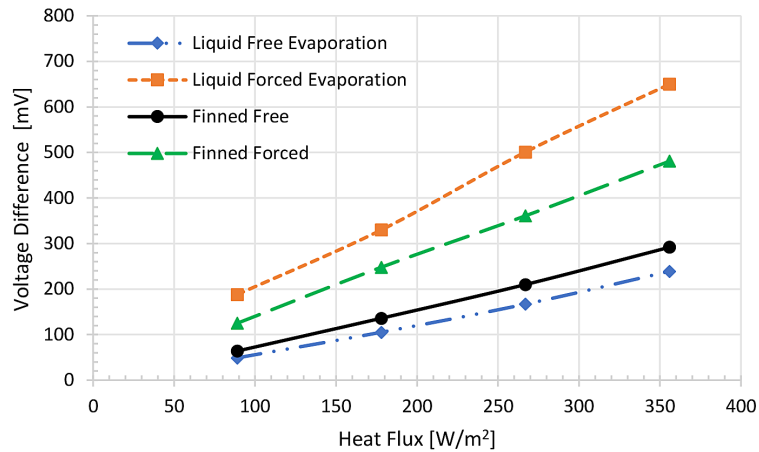


Figure 12. Comparison between the voltages generated by the different methods

CONCLUSIONS

This study outlined an experimental investigation of incorporating evaporation of liquids into thermoelectric generators based on heat transfer to improve its efficiency. Three different scenarios were implemented to prove its efficiency, which are: (i) free and forced convection heat transfer from the TEG to show temperature distribution and voltage difference; (ii) TEG integrated with fins to visualize the effect of finned in both free and forced modes; the last one (iii) utilized free and forced Liquid Evaporation convection modes on the temperature distribution and voltage difference for TEG. The findings of this study can be summarized as follows:

When compared to the free convection, the forced convection will improve the TEG voltage variation by 116.5%.

When compared to the free convection without fins, the free and forced convection with finned improved the voltage variation of TEG by 119.8% and 288.4%, respectively. Furthermore, as compared to free convection with fins, the forced convection with fins will improve the TEG voltage variation by 78.6%.

When compared to the free convection without fins, the free and forced liquid evaporation convection will improve the voltage variation of TEG by 73.8% and 435.9%, respectively. Furthermore, as compared to the free liquid evaporation convection, forced liquid evaporation convection improved TEG voltage variation by 217.3%.

This research will be used as a reference for future thermoelectric generator strategies to achieve optimal performance.

Acknowledgments

The authors appreciate the financial support provided by Applied Science Private University and Tafila Technical University, Jordan.

REFERENCES

1. Angeline A.A., Jayakumar J., Asirvatham L.G. 2017. Performance analysis of $(\text{Bi}_2\text{Te}_3\text{-PbTe})$ hybrid thermoelectric generator. *International Journal of Power Electronics and Drive System*, 8(2), 917–925.
2. Araiz M., Casi Á., Catalán L., Martínez Á., Astrain D. 2020. Prospects of waste-heat recovery from a real industry using thermoelectric generators: Economic and power output analysis. *Energy Convers Manag*, 205, 112376.
3. Araiz M., Casi Á., Catalán L., Aranguren P., Astrain D. 2021. Thermoelectric generator with passive biphasic thermosyphon heat exchanger for waste heat recovery: Design and Experimentation. *Energies*, 14, 5815.
4. Aridi R., Faraj J., Ali S., Lemenand T., Khaled M. 2021. Thermoelectric power generators: State-of-the-art. *Heat Recovery Method, and Challenges. Electricity*, 2, 359–386.
5. Atouei S.A., Ranjbar A.A., Rezaia A. 2017. Experimental investigation of two-stage thermoelectric generator system integrated with phase change materials. *Appl Energy*, 208, 332–343.
6. Bergman T.L., Incropera F.P., DeWitt D.P., Lavine A.S. 2011. *Fundamentals of heat and mass transfer*. John Wiley & Sons.
7. Børset M.T., Wilhelmsen Ø., Kjelstrup S., Burheim O.S. 2017. Exploring the potential for waste heat recovery during metal casting with thermoelectric

- generators: On-site experiments and mathematical modeling. *Energy*, 118, 865–875.
8. Cao Q., Luan W., Wang T. 2018. Performance enhancement of heat pipes assisted thermoelectric generator for automobile exhaust heat recovery. *Appl Therm Eng*, 130, 1472–79.
 9. Chen J., Li K., Liu C., Li M., Lv Y., Jia L., et al. 2017. Enhanced efficiency of thermoelectric generator by optimizing mechanical and electrical structures. *Energies*, 10, 1329.
 10. Churchill S.W., Chu H.H.S. 1975. Correlating equations for laminar and turbulent free convection from a vertical plate. *Int J Heat Mass Transf*, 18, 1323–29.
 11. Dai D., Zhou Y., Liu J. 2011. Liquid metal based thermoelectric generation system for waste heat recovery. *Renew Energy*, 36, 3530–36.
 12. Dell R., Petralia M.T., Pokharel A., Unnthorsson R. 2019. Thermoelectric generator using passive cooling. *Adv Thermoelectr Mater Energy Harvest Appl*, 63.
 13. Elsheikh M.H., Shnawah D.A., Sabri M.F.M., Said S.B.M., Hassan M.H., Bashir M.B.A., et al. 2014. A review on thermoelectric renewable energy: Principle parameters that affect their performance. *Renew Sustain Energy Rev*, 30, 337–355.
 14. Hadjistassou C., Kyriakides E., Georgiou J. 2013. Designing high efficiency segmented thermoelectric generators. *Energy Convers Manag*, 66, 165–172.
 15. Jaziri N., Boughamoura A., Müller J., Mezghani B., Tounsi F., Ismail M. 2020. A comprehensive review of Thermoelectric Generators: Technologies and common applications. *Energy Reports*, 6, 264–287.
 16. Meng F., Chen L., Feng Y., Xiong B. 2017. Thermoelectric generator for industrial gas phase waste heat recovery. *Energy*, 135, 83–90.
 17. Snyder G.J., Toberer E.S. 2011. Complex thermoelectric materials. *Mater Sustain Energy a Collect Peer-Reviewed Res Rev Artic from Nat Publ Gr*, 101–110.
 18. Omer S.A., Infield D.G. 1998. Design optimization of thermoelectric devices for solar power generation. *Sol Energy Mater Sol Cells*, 53, 67–82.
 19. Orr B., Akbarzadeh A., Mochizuki M., Singh R. 2016. A review of car waste heat recovery systems utilising thermoelectric generators and heat pipes. *Appl Therm Eng*, 101, 490–495.
 20. Polozine A., Sirotinskaya S., Schaeffer L. 2014. History of development of thermoelectric materials for electric power generation and criteria of their quality. *Mater Res*, 17, 1260–67.
 21. Shittu S., Li G., Zhao X., Ma X. 2019. Series of detail comparison and optimization of thermoelectric element geometry considering the PV effect. *Renew Energy*, 130, 930–942.
 22. Rea J.E., Oshman C.J., Singh A., Alleman J., Parilla P.A., Hardin C.L., et al. 2018. Experimental demonstration of a dispatchable latent heat storage system with aluminum-silicon as a phase change material. *Appl Energy*, 230, 1218–29.
 23. Wang T., Luan W., Liu T., Tu S-T., Yan J. 2016. Performance enhancement of thermoelectric waste heat recovery system by using metal foam inserts. *Energy Convers Manag*, 124, 13–19.